Microdeformation Mechanisms in Propylene–Ethylene Block Copolymer

KOSEI HAYASHI,* TETSUYA MORIOKA, and SHIGEYUKI TOKI

Tonen Chemical Corp., Nishitsurugaoka-1, Ohi-machi, Iruma-gun, Saitama 354, Japan

SYNOPSIS

Blends of propylene–ethylene block copolymer (PEB) and propylene homopolymer (PP) were prepared to give various rubber contents (4–20 wt %). By diluting the PEB with PP with molecular weight equal to that of the PEB matrix, molecular characteristics of all the blends were kept constant. The rubber particle size and size distribution of all the blends were almost constant, so that the interparticle distance decreased with increased rubber content. According to the observation of the fracture behavior at −20°C, a brittle to ductile transition was found at the rubber content of 16 wt %. Microdeformation behavior of the blends was investigated in the region of brittle to ductile transition by using transmission electron microscopy. In the case of the brittle sample with low rubber content, crazing and voiding were observed. Whereas even in the ductile sample with high rubber content, crazing certainly took place before shear yielding. The origin of ductile fracture could possibly be attributed to the relaxation of strain constraint by the microvoids contained in the craze.

INTRODUCTION

A number of multiphase polymer alloys have been developed and commercialized extensively because of good mechanical properties, such as high modulus, high impact strength, good heat resistance, and so on.

It is well known that rigid polymer itself can be toughened if many fine rubber particles are dispersed in the matrix. The toughening mechanisms of such systems have been widely investigated by many researchers and attributed to two deformation mechanisms, crazing and shear yielding. In general, polymers composed of brittle matrix [e.g., high impact polystyrene (PS)] are found to dissipate the impact energy by microcrazing.[1–4] On the other hand, polymers with ductile matrix (e.g., rubber-toughened nylon) favor shear yielding because the cavitation of the rubber particles causes successive relaxation of the strain constraint between particles.[5,6]

Although many studies on the fracture mechanisms in the amorphous or ductile polymer systems are presented, there are not many works on polyolefin systems.

In polypropylene (PP)/rubber blends, both crazing and shear yielding are reported by some researchers. Jang et al.[7–8] indicated that crazing dominantly occurred if dispersed rubber particle size was large, while shear yielding would be induced if particle size was small (below 0.5 μm). Chou et al.[9–10] also described that PP/EPR blends showed brittle to ductile (B–D) transition with varying temperature, strain rate, and blend composition. Although the fracture behaviour in rubber-modified PP have been demonstrated by these authors, the mechanism of B–D transition is still uncertain. The objective of the present study is to investigate the toughening mechanism and its dependency on the rubber content of propylene–ethylene block copolymers (PEBs).

EXPERIMENTAL

Sample Preparation

In order to make a series of PEBs containing different amount of rubber particles, PEBs were diluted

* To whom correspondence should be addressed.

Journal of Applied Polymer Science, Vol. 48, 411–418 (1993)
 CCC 0021-8995/93/030411-08

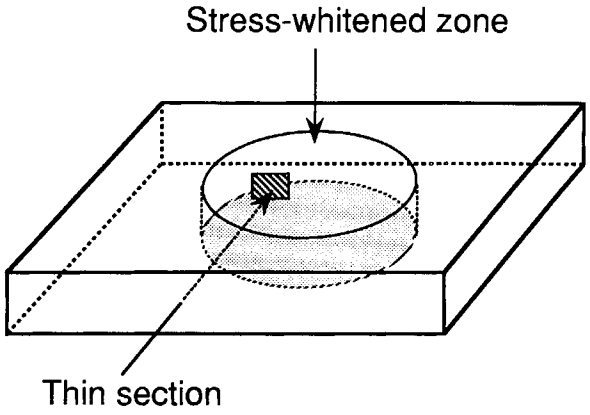

Figure 1 DuPont impact-tested piece for TEM observation.

with various amount of homo PP. The reason blends were made with PEB and PP instead of PP and ethylene–propylene rubber (EPR) was to achieve uniform dispersion of rubber particles.

PEB as the parent material was an experimental resin including approximately 20 wt % of rubber. The molecular weight (M_w) of matrix and rubber phase was 290,000 and 460,000, respectively. Homo PP mixed with PEB was also an experimental resin with molecular weight of 290,000, equal to that of the matrix of PEB. Pellets of the two polymers were first dry blended to give rubber contents of 4–20 wt %, then melt blended in a Brabender-type mixer operating at a screw speed of 150 rpm with barrel temperature set at 170°C. The parent PEB alone was also kneaded with the same conditions. The blends thus prepared were compression moulded at 210°C for material testing and morphology observations.

Material Testing

Falling weight impact test was carried out according to JIS K7211, using a DuPont impact testing machine at −20°C. Sample dimensions were 50 mm × 50 mm × 1 mm. Flexural modulus values were measured following JIS K7203.

Morphology Observations

Scanning electron microscope (SEM) and transmission electron microscope (TEM) were used to examine the morphology of PEB samples. SEM was used for the particle-size determination. The microtomed smooth surface was etched with hot xylene to remove the rubber component, then the surface was coated with a gold–palladium alloy. The rubber particle size and size distribution were calculated using a Luzex 500 (NIRECO) image processor.

TEM was also used to examine the change of internal microstructure induced by the impact force. The center of the stress-whitened area was chosen for the observation as shown in Figure 1. After staining with RuO_4 vapour for a few hours, a thin section of 80 nm was cut perpendicular to the sheet plane.

RESULTS AND DISCUSSION

Blend Morphology

When a flat surface is made by a microtome for the SEM analysis, the plane does not always run through the center of the particles. Therefore, the particle size obtained from the SEM micrograph was corrected to give the real particle size.[11] In image analysis, particles with diameter below 0.1 μm were not counted. This would not be a problem in discussing the impact properties of the blends. The area-average particle size is plotted against the rubber content as shown in Figure 2. The particle sizes of all the blends are nearly constant (approximately 1.8 μm). This means that the mixing process and moulding step caused neither a further reduction nor coalescence of the particles. It is considered that the mixing energy is sufficient for rubber particles to be reduced to the equilibrium state.

Particle-size distributions of blends containing 6, 16, and 20 wt % of rubber are shown in Figure 3. Plots of cumulative number fraction of particles against logarithmic rubber-particle diameter for

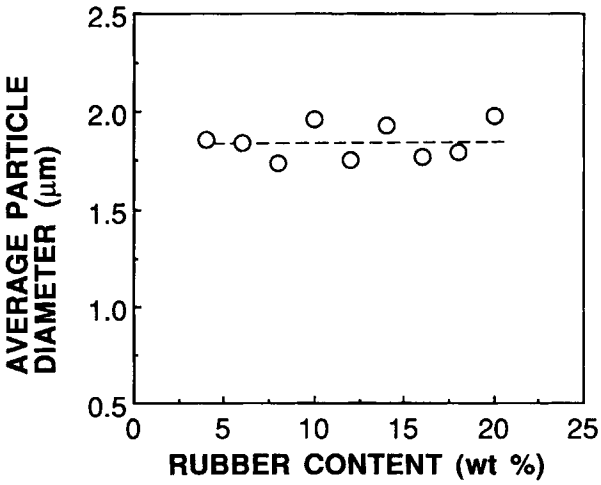

Figure 2 Plots of average particle diameter against rubber content.

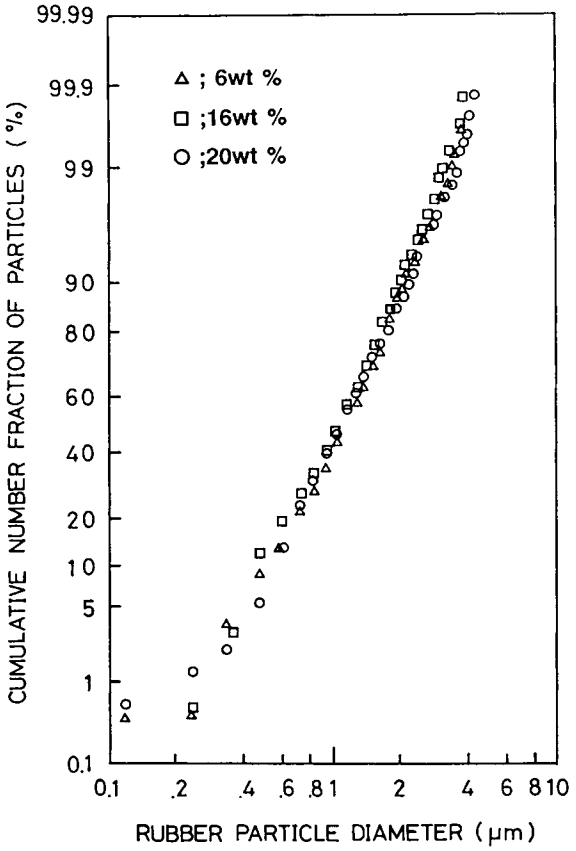

Figure 3 Log-normal distribution plot of rubber particle diameter.

these three blends fit a straight line. This implies the particle-size distribution obeys the log-normal distribution. As the particle-size distributions are the same in each case, all the blends are assumed to have equivalent size distribution.

From these morphological examinations, it is concluded that the only difference among the samples of different rubber content is interparticle distance (ID). Although the substantial ID is not obtained without taking into account the three-dimensional arrangement of the particles, apparent interparticle distance (AID) was calculated by assuming that the particles are arranged in a cubic lattice:

$$\mathrm{AID} = d[(\pi/6\phi)^{1/3} - 1]$$

where d is the average particle size and ϕ is the rubber volume fraction.

In Figure 4, AID value is plotted against rubber content. The AID decreases with increasing rubber content.

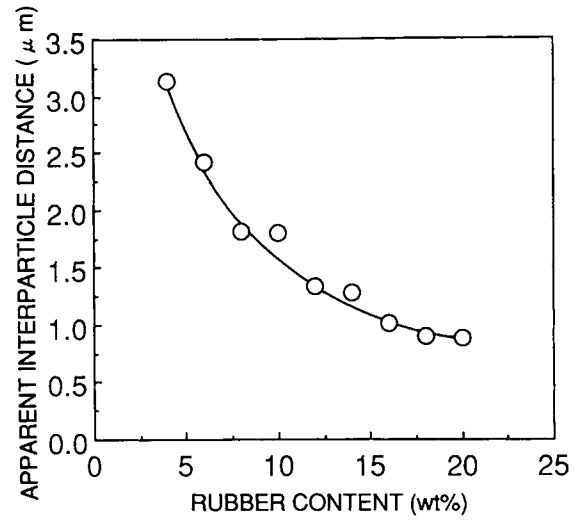

Figure 4 Plots of apparent interparticle distance against rubber content.

Impact Strength and Modulus

DuPont impact strength of the blends measured at −20°C is given in Figure 5. With increasing rubber content, impact strength increases gradually to 14 wt %. In this region the specimens break in a brittle manner. At 16 wt %, however, impact strength increases dramatically, and deformation behavior changes from brittle to ductile. Above 18 wt % the blends are very tough, where the specimens are yielded and punctured by the striker.

In Figure 6, the flexural modulus is plotted against the rubber content. The flexural modulus decreases linearly with rubber content. This indicates that the characteristics of the matrix are not affected by the amount of rubber phase.

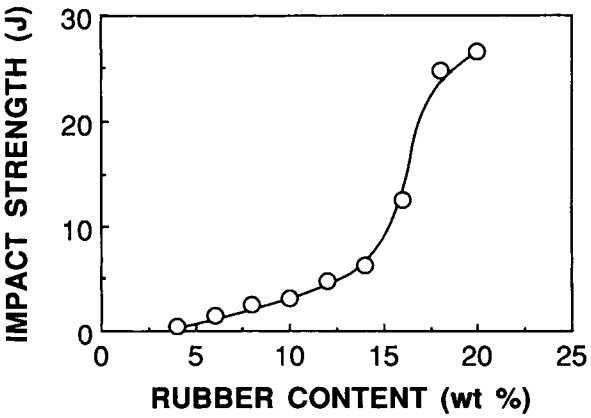

Figure 5 DuPont impact strength at −20°C versus rubber content.

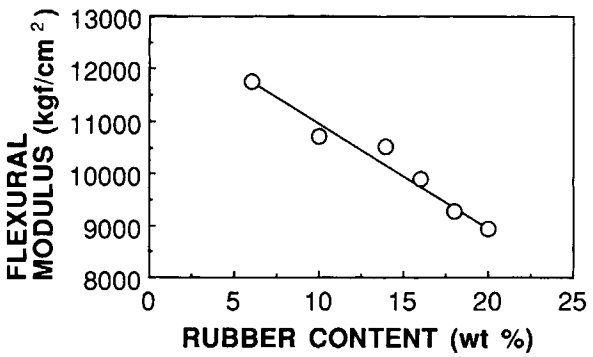

Figure 6 Flexural modulus versus rubber content.

Microdeformation Behavior

In the examination of the microstructure of the impact-tested pieces, TEM provides more exact information than SEM because not only the rubber phase but also the craze can be observed by using the RuO_4 staining method.[12] In Figure 7 the internal morphologies of the blends that underwent the stress just before the fracture stress are shown. Figure 7(a) is a TEM micrograph of the blend containing 6 wt % rubber, which exhibits brittle fracture. A few thin crazes can be observed at the particles with adequate particle diameter. No crazes are generated from fine particles. The shape of the particles is almost spherical, that is, there is no apparent change in shape as compared with that of the undeformed sample. This suggests that the deformation is attributed only to matrix crazing. Therefore, brittle fracture will occur with the breakdown of craze when the stress at the tip of the craze exceeds fibril-rupture stress. The voiding in the rubber particle was scarcely observed at this rubber content. Thus, it is concluded that crazing of PP matrix can occur without voiding of rubber.

Figure 7(b) shows the microdeformation of blend containing 16 wt % rubber. This sample lies in the transition region from brittle to ductile. The crazes that grew both in length and thickness are visible in comparison with the brittle sample [Fig. 7(a)]. Rubber particles are deformed in the direction parallel to the applied stress. Although an apparent shear band is not visible in the TEM micrograph, large deformation of rubber particles suggests that matrix yielding occurs as well as crazing.

In the case of the blends containing 20 wt % rubber, largely elongated rubber domains are observed [Fig. 7(c)], though the original rubber domain is nearly spherical. This dramatic morphological alteration suggests that matrix shear yielding has occurred as a result of large-impact energy dissipation. The voiding has also taken place. Some of the voids would, however, be interfacial debonding at the poles of the particle in the stretched direction. In this sample distinct crazes such as in the brittle (6 wt %) or semi-ductile (16 wt %) sample are no longer visible.

From these morphological observations, there were significant differences in microdeformation behaviour of PEBs depending on their rubber contents. As generally recognized, B–D transition is based on the change in deformation mode from crazing to shear yielding.

So far we have observed the final morphology formed when the sample experienced the highest stress just below fracture stress. However, it was necessary to investigate how the deformation proceeded during the plastic deformation. To hold the specimen in the intermediate state of the deformation, the applied impact energy was varied. By altering the height of the weight in the impact test, the deformation was regarded as the intermediate state.

Figure 8 shows the morphology change of the ductile sample that contains 20 wt % of rubber. When the applied stress was far below the fracture stress, crazing was observed [Fig. 8(a)]. Since the shape of the particle is spherical, the same as that of the untested sample, no shear yielding took place at this stage. Even in a ductile sample, the crazing process contributes to energy dissipation in the early stage of deformation. The voiding was also observed in some particles.

By increasing the applied stress, the number of crazes generated at each particle became larger [Fig. 8(b)]. Deformation of the particles was also observed mainly in the relatively large particles that formed a large number of crazes. This suggests that the region around the larger particle has caused shear yielding. Therefore, both crazing and shear yielding occur at the same time. The voiding in the rubber particle was observed as well as in Figure 8(a).

The later stage of the deformation is shown in Figure 8(c). The largely extended particles as previously seen in Figure 7(c) were observed. Furthermore, the voids were observed in several places, and happened during the crazing and the shear yielding.

With the deformed rubber particles the traces of craze were recognized. Therefore, in the ductile sample the microdeformation mode changed from crazing to shear yielding during the deformation.

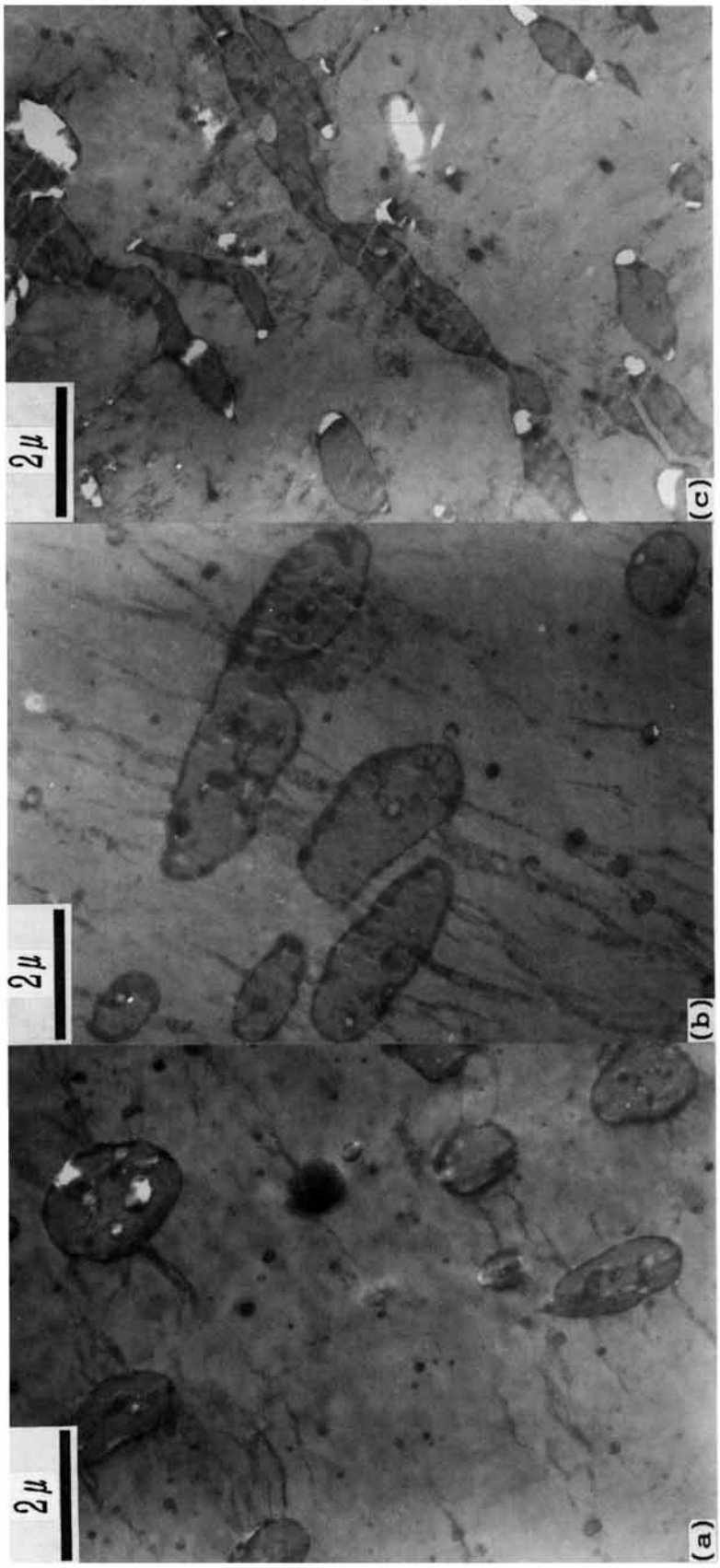

Figure 7 Transmission electron micrographs of stress-whitened zone. The rubber content is (a) 6 wt %, (b) 16 wt %, and (c) 20 wt %. To each specimen was applied the maximum energy just below the fracture energy.

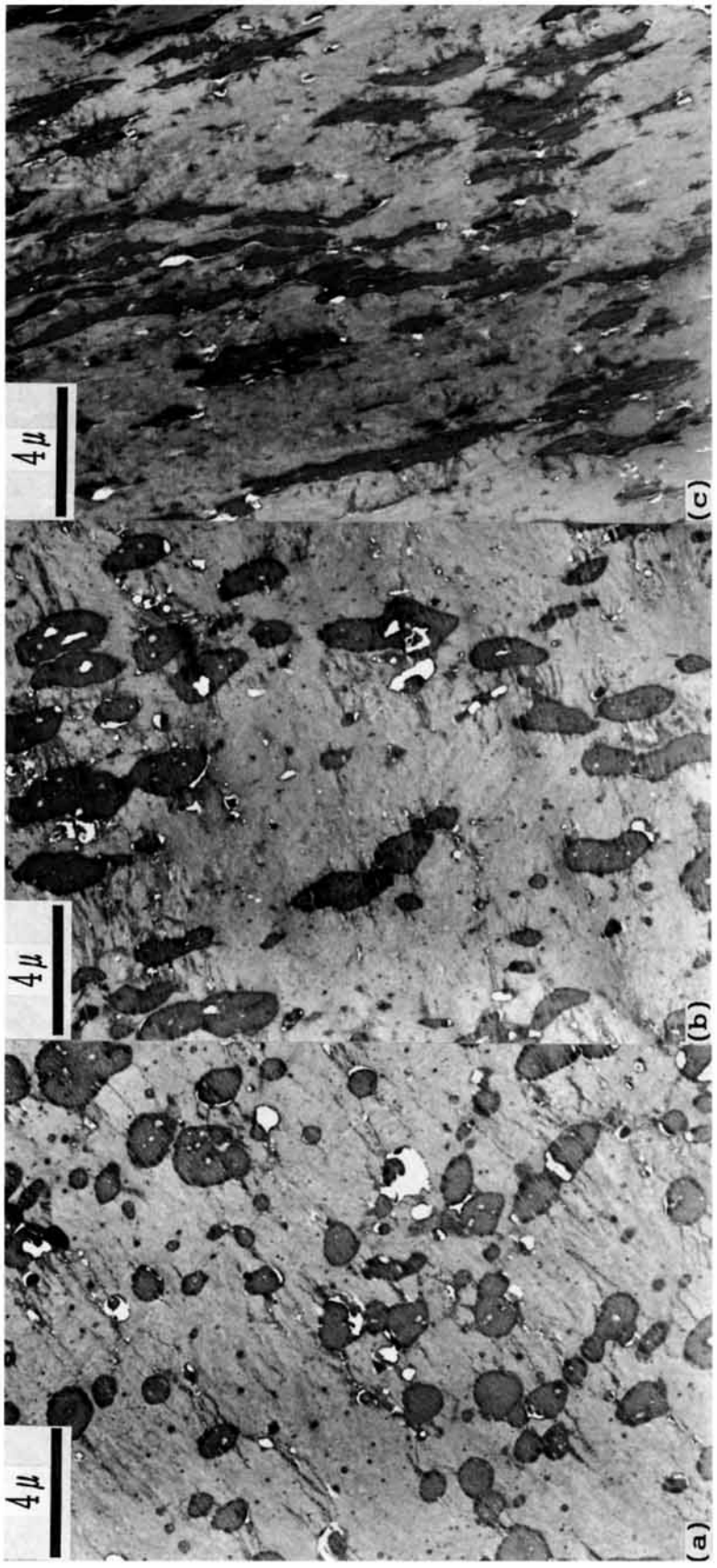

Figure 8 Transmission electron micrographs showing the microdeformation process of PEB containing 20 wt % of rubber. The applied impact energy level was varied by controlling the height of the weight: (a) 5 J, (b) 10 J, and (c) 20 J.

Brittle–Ductile Transition

We now consider the origin of B–D transition from morphological points of view. In Figure 9 the DuPont impact strength (DIS) is plotted against the AID. DIS is in good agreement with ID. When the ID is decreased below 1 μm, the DIS increases dramatically.

Wu[13,14] recently demonstrated that in rubber-toughened nylon the interparticle distance is the only parameter that determines whether the blend is brittle or ductile. It is also suggested that in PEB AID is an important factor that controls toughness.

The B–D transition has generally been ascribed to an alteration of stress state. According to Wu,[14] the blends are ductile when ID is less than a critical length, because the thinner ligaments can readily yield in the plane stress state.

It is well known that microdeformation behaviour is influenced by many factors, such as temperature, strain rate, sample geometry, and so on. If these testing conditions are constant, matrix ductility is an important factor that affects the microdeformation mode. In a ductile matrix such as nylon, the shear yielding is the primary energy-dissipation mode. Cavitation of rubber particles also takes place so that the matrix yielding is promoted without causing a crack. On the other hand in brittle matrix such as PP and PS, crazing can easily be initiated. Narisawa et al.[15] explained that the ratio of crazing stress and shear-yielding stress is an important factor that determines whether material is brittle or ductile. In the case of PP, Ishikawa and Narisawa[16] have shown that crazing can be generated without forming a local plastic zone at the tip of the notch in a three-point bending test of a round notched bar. This result is consistent with the crazing behaviour in PEB. Crazes are generated at the interface of rubber particle and PP matrix in each rubber content.

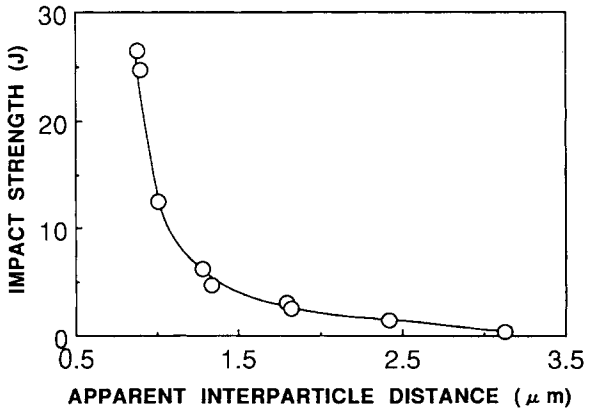

Figure 9 DuPont impact strength versus apparent interparticle distance.

Voiding of the rubber particle was also observed in all the rubber content. However, correlation between the voiding and the impact properties was not clear in PEB. Since the matrix of the blends is quite brittle, it would not yield even when the AID is approximately 1 μm. Brittle matrix, however, tends to craze easily.

On the basis of the experimental results, it may be concluded that crazing can occur independently of AID. Thus, impact energy is mainly dissipated by crazing in the brittle sample (low rubber content) and even in the early period of the ductile sample (high rubber content). However, in the later stage of ductile fracture, the shear yielding took place. This suggests that the stress field changes from the plane–strain to plane–stress during the deformation.

These microdeformation mechanisms can be explained as follows. As the impact force is applied, the crazes are first nucleated at the particles, independent of AID. If the AID is long enough (less rubber content), the stress field is scarcely affected by the neighbouring particle. So the external load required for craze initiation is higher than that in the case of shorter AID. Since the density of craze nucleation site is low, the stress at the tip of the craze can readily exceed the stress that is needed for crack initiation. Thus, the low rubber-content sample fractures in a brittle manner without showing further ductility of the PP matrix. On the other hand, as the AID is shorter, the influence of stress fields induced by the neighbouring particles grows greater.[17] Thus, the crazes can be generated with a lower external load. Increasing load will make the crazes grow and additional crazes are formed from the same particle. This multiple craze formation is probably due to the interaction of stress field. The stress around the particle is decreased by the multiple-craze formation. So the stress at the tip of the craze is maintained below crack initiation stress. The region between the particles is consequently filled with numerous microvoids contained in those crazes. So the constraint of the transverse strain between neighbouring particles is relaxed. Consequently, the ligaments where the craze has sufficiently developed can deform in the plane–stress state. Such a deformed zone spreads over a wide region and a catastrophic crack will be prevented. Then the ductile fracture is caused by the chain scission of the yielded zone. Therefore, in the ductile sample of PEB, not only the crazing in the early stage of deformation, but also shear yielding contributes to the dissipation of the impact energy.

CONCLUSIONS

Microdeformation mechanisms of PEB have been revealed in both brittle and ductile fractures. In the brittle region, the microdeformation mode was crazing and voiding. However, in the ductile region, the deformation mode changed from crazing with voiding in the early stage of deformation to shear yielding in the later stage of deformation. The relaxation of strain constraint by the microvoids contained in the craze contributes to the transition of the deformation mode.

REFERENCES

1. C. B. Bucknall and R. R. Smith, *Polymer,* **6,** 437 (1965).
2. R. P. Kambour and R. R. Russell, *Polymer,* **12,** 237 (1971).
3. S. G. Turley and H. Keskkula, *Polymer,* **21,** 466 (1980).
4. A. M. Donald and E. Kramer, *J. Appl. Polym. Sci.,* **27,** 3729 (1982).
5. R. J. M. Borggreve, R. J. Gaymans, J. Schuijer, and J. F. Ingen Housz, *Polymer,* **28,** 1489 (1987).
6. S. Wu, *J. Polym. Sci., Polym. Phys. Ed.,* **21,** 699 (1983).
7. B. Z. Jang, D. R. Uhlmann, and J. B. Vander Sande, *Polym. Eng. Sci.,* **25,** 643 (1985).
8. B. Z. Jang, D. R. Uhlmann, and J. B. Vander Sande, *J. Appl. Polym. Sci.,* **29,** 3409 (1984).
9. C. J. Chou, K. Vijayan, D. Kirby, A. Hiltner, and E. Baer, *J. Mater. Sci.,* **23,** 2521 (1988).
10. C. J. Chou, K. Vijayan, D. Kirby, A. Hiltner, and E. Baer, *J. Mater. Sci.,* **23,** 2533 (1988).
11. L. Holliday, *Composite Materials,* Elsevier, Amsterdam, 1966, p. 21.
12. H. Sano, T. Usami, and H. Nakagawa, *Polymer,* **27,** 1497 (1986).
13. S. Wu, *Polymer,* **26,** 1856 (1985).
14. S. Wu, *J. Appl. Polym. Sci.,* **35,** 549 (1988).
15. I. Narisawa, M. Ishikawa, T. Murayama, and H. Ogawa, *Kobunshi Ronbunshu,* **36**(8), 543 (1979).
16. M. Ishikawa, and I. Narisawa, *Polym. Prepr. Jpn.,* **33,** 2379 (1984).
17. M. Matsuo, Tsuey T. Wang, and T. K. Kwei, *J. Polym. Sci., A-2,* **10,** 1085 (1972).

Received June 11, 1992
Accepted July 25, 1992